

Mode Competition and Control in Free-Electron-Laser Oscillators

Thomas M. Antonsen, Jr.,^(a) and Baruch Levush

Laboratory for Plasma Research, University of Maryland, College Park, Maryland 20742

(Received 3 October 1988)

The problem of longitudinal-mode competition in free-electron lasers is addressed. It is shown that for small enough ratios of the current to the output coupling coefficient many single-mode states are possible. However, the time required to reach these states becomes extremely long for typical devices. Before reaching a single-mode state the radiation field becomes relatively constant in amplitude with modulations of its phase. Finally, a simple method for reaching the stable single-mode state with maximum efficiency is suggested.

PACS numbers: 42.55.Tb

One of the most important problems in the operation of high-power generators of coherent radiation is the competition of the many eigenmodes of the resonator for the beam energy.^{1,2} This paper addresses the effect of multimode interaction on the operation of a free-electron-laser (FEL) oscillator fed by a continuous electron beam.¹ Our principal results are a determination of the circumstances under which single-mode operation can be achieved and a description of a method of controlling the detuning of the final mode. In addition, we present a description of the process by which single-model operation results during the transient start-up phase of the oscillator.

The model we consider is the simplest one which retains the effects of mode competition; namely, the one-dimensional, low-gain oscillator.¹ In this model the radiation field in the resonator can be expressed as a superposition of empty cavity modes whose amplitudes and phases change slowly in time (compared with the transit time of the electrons through the interaction region) due to their interaction with the beam. We further assume that the electrons' energies change only slightly on transiting the device. This allows us to use a pendulum equation to describe the particle motion in the ponderomotive potential well of the beat wave.

With these approximations the characteristics of the operation of an oscillator in a single mode are determined by two parameters: The first is the normalized detuning

$$p_{\text{inj}} = [(k_w + k)v_{\text{inj}} - \omega]T, \quad (1)$$

where k_w and k are the wiggler and radiation wave numbers, v_{inj} is the value of the axial velocity of the electron beam (here assumed to be monoenergetic) as it enters the interaction region, ω is the frequency of the radiation, and $T=L/v_{\text{inj}}$ is the transit time of the particles through the interaction region whose length is L .

The second parameter measures the strength of the radiation field and is given by

$$a_0 = \omega_s^2 T^2, \quad (2)$$

where ω_s is the synchrotron frequency for a particle at

the bottom of the ponderomotive potential well.³ As mentioned, these two parameters determine the characteristics of an oscillator operating in a single mode. For example, the dimensionless efficiency⁴ Δp in the small-signal limit is given by $\Delta p = a_0^2 G(p_{\text{inj}})$, where $G(p_{\text{inj}}) = p_{\text{inj}}^{-3} [1 - \cos p_{\text{inj}} - (p_{\text{inj}}/2) \sin p_{\text{inj}}]$ is the gain function⁵ whose maximum value 0.069 occurs at a detuning $p_{\text{inj}} = 2.606$. In the nonlinear regime the dimensionless efficiency maximizes at a value 5.5 when $p_{\text{inj}} = 5.14$ and $a_0 = 18.0$ corresponding to the situation where particles execute approximately half a bounce in the ponderomotive well.

The preceding discussion is based on the assumption of single-mode operation with a specified frequency ω and wave number k such that the detuning p_{inj} is determined. In a low-gain oscillator the frequency and wave number must correspond approximately to a cavity mode. These are determined by quantizing the axial wave number $k_n = k_0 + n\pi/L_c$ and $\omega_n = \omega_0 + n\pi v_g/L_c$, where $n = 0, \pm 1, \pm 2$ labels the mode, ω_0 and k_0 are the frequency and wave number of some arbitrarily chosen reference mode, v_g is the axial group velocity of the radiation, L_c is the cavity length, and we have assumed uniform spacing of modes. Thus, for a given injection velocity each mode has its own detuning parameter defined by Eq. (1),

$$p_{\text{inj},n} = p_{\text{inj},0} - \epsilon\pi n, \quad (3)$$

where $p_{\text{inj},0}$ is the detuning for the $n=0$ mode and

$$\epsilon = \frac{L}{L_c} \left[\frac{v_g}{v_{\text{inj}}} - 1 \right] \quad (4)$$

is the slippage parameter which is usually small. The number of modes N which will compete for the beam's energy can be estimated by determining the number of modes with detunings under the positive portion of the gain function G , $N \sim \epsilon^{-1}$.

We can now simulate the competition of many modes by the following procedure.^{1,2} Because of the low gain and correspondingly small losses, the radiation field in the resonator can be represented as a superposition of cavity modes with amplitudes and phases which evolve slowly due to their interaction with the particles. The

field amplitude and phase at any point will be nearly periodic in time with a period equal to the round-trip travel time of radiation in the cavity, which we assume to be much smaller than the time scale over which the amplitudes change. We may then numerically integrate the pendulum equation for an ensemble of particles with beat-wave phase ψ and entrance time t_0 uniformly distributed over the intervals $[0, 2\pi]$ and $[0, 2]$, respectively, so that

$$\frac{dp}{d\xi} = \frac{d^2\psi}{d\xi^2} = \text{Im} \left[\sum_n a_n \exp\{i[\psi - n\pi(\epsilon\xi + t_0)]\} \right], \quad (5)$$

where $\xi = z/L$ measures distance through the interaction region, $\psi = (k_w + k_0)z - \omega_0 t$ is the particle's phase, p is proportional to the energy deviation of the particle, $p(\xi) = [(k_0 + k_w)v_z(\xi) - \omega_0]T$ with $p(\xi=0) = p_{\text{inj},0}$, and we have normalized t_0 such that radiation travels the length of the resonator in one unit of time.

The quantity a_n is the complex amplitude of the n th mode normalized in the same way as a_0 , and it depends on a slow time variable τ_s normalized to the decay time of radiation in the empty cavity. Thus the field at the entrance to the interaction region has the multiple time-scale representation $a(\tau_s, t_0) = \sum_n a_n(\tau_s) \exp(-in\pi t_0)$. The evolution of a_n is described by the equation

$$\left(\frac{d}{d\tau_s} + \frac{1}{2} \right) a_n(\tau_s) = -\frac{i\hat{I}}{4v} \int_0^2 \frac{d\tau_0}{2} \int_0^1 d\xi \langle \exp\{-i[\psi - n\pi(\epsilon\xi + t_0)]\} \rangle, \quad (6)$$

where \hat{I} is a normalized current,⁶ $2v$ is the fraction of radiation power extracted (including losses) per pass, and the angular average representing the projection of the beam current on the n th mode is over initial entrance phases of the particles. In this model we have assumed that all cavity modes have the same damping rate, which in normalized units is $\frac{1}{2}$.

The previously discussed single-mode theory is obtained from this model by including only the $n=0$ mode. One then obtains from the particle equations the average energy extraction $\Delta p = p_{\text{inj},0} - \langle p(\xi=1) \rangle$ and from the wave equation, or equivalently from energy balance, the current needed to maintain the mode in steady state. This information is displayed in Fig. 1 where level curves of energy extraction Δp (solid curves) and beam current (dashed curves) are plotted in the $(a_0, p_{\text{inj},0})$ plane. In the plot, beam current is normalized to the minimum value required to start oscillations in the cavity, $\chi = \hat{I}/\hat{I}_{\text{start}}$ where $\hat{I}_{\text{start}} = 2v/G(2.606) \approx 29v$.

The stability of single-mode equilibria to the growth of side bands was determined for the given model [Eqs. (5) and (6)] in Ref. 7. The result is shown in Fig. 1. Single-frequency equilibria are stable within the triangular-shaped region of the (a_0, p_{inj}) plane. The procedure used in Ref. 7 was to assume a single-frequency equilibrium was present (a_0, p_{inj}) which was linearly per-

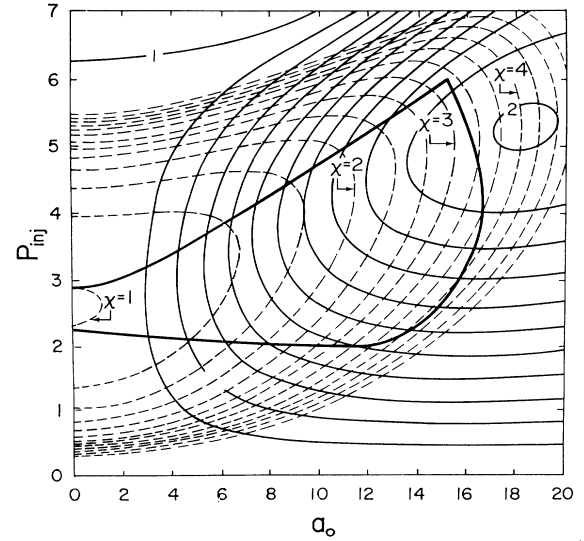


FIG. 1. Solid lines are the equal energy extraction (Δp) curves in the (p_{inj}, a_0) plane. The curve labeled 1 corresponds to $\Delta p = 0$, the curve 2 corresponds to $\Delta p = 5.5$. The difference between the neighboring level curves is 0.5. The dashed lines are the level curves of \hat{I}/v , which is obtained from the energy balance at a particular value of a_0 and p_{inj} . The numbers on the curve indicate the value of $\chi = \hat{I}/\hat{I}_{\text{start}}$. Only inside of the triangular-shaped region is the stable single-mode operation possible.

turbed by small-amplitude satellites a_n ($n \neq 0$). Satellites with equal values of $|n|$ couple linearly, yielding a quadratic dispersion relation for growth rate as a function of satellite mode number. The coefficients in the dispersion relation were determined numerically by integrating particle orbits, and the parameter values for which all satellites were stable were recorded. The particular plot in Fig. 1 is for $\epsilon = 0.2$. For smaller values of ϵ the plot would appear essentially the same except that the band of stable p_{inj} values at $a_0 = 0$ would shrink to a point centered at $p_{\text{inj}} = 2.606$.

A number of important points are to be learned by examining Fig. 1. The first is that the single-mode equilibrium with maximum efficiency occurring for $p_{\text{inj}} \approx 5.14$ and $a_0 = 18$ is not stable. One would expect to reach this equilibrium by setting the current ratio $\chi = \hat{I}/\hat{I}_{\text{start}}$ to 4. The results of simulations show instead that the system settles to a single-mode equilibrium with $p_{\text{inj}} \approx 2.6$ and $a_0 = 14$, which is just inside the stable region with $\chi = 4$. (Simulations show for higher values of current no stable single-mode equilibria are possible¹ due to the excitation of the side-band instability.^{8,9}) The second point is that if one now considers stable single-mode equilibria, the maximum efficiency is achieved for an equilibrium with $a_0 = 15.2$, $p_{\text{inj}} = 5$, and $\chi \sim 3$. However, with $\chi = 3$ there is a range of values of p_{inj} falling in the stable triangle. Thus, if ϵ is small there are many different stable single-mode equilibria corresponding to the different detunings

of the many possible cavity modes [cf. Eq. (3)] in this range. Therefore, the question arises as to which single-mode equilibrium state the system will evolve.

To answer this question we have turned to a numerical simulation of Eqs. (5)–(7). A small noise source term¹⁰ was added to provide a “seed” signal for each mode.⁷ Further, to simulate the effect of the time dependence of the voltage pulse in our model we allow $P_{inj,0}$ to become a function of the slow time variable τ_s . Because the FEL resonance is narrow only the last few percent of the voltage rise, corresponding to values of p_{inj} of order π , affect the final mode. (The interaction is less sensitive to small changes in current so we fix its value.) We thus take as a model for $p_{inj,0}(\tau_s)$ a hyperbola characterized by the parameters p_f , p_s , p_* , and τ_{sw}

$$[p_{inj,0}(\tau_s) - p_f - p_s(\tau_s - \tau_{sw})][p_{inj,0}(\tau_s) - p_f] = p_*^2.$$

The time dependence is such that $p_{inj,0}$ increases initially linearly with time at a rate p_s and makes a transition at about $\tau_s = \tau_{sw}$ to a constant value p_f . The abruptness of the transition is controlled by the parameter p_* .

The time history of the energy extracted as well as the spectrum of mode amplitudes at $\tau_s = 60$ and the fast time dependence of the output power (averaged over a wave period) at $\tau_s = 60$ are shown in Fig. 2 for a sample run. The parameters for this simulation are $\epsilon = 0.05$, $p_* = 4.5$, $p_s = 1$, and $\tau_{sw} = 20$. As can be seen, the energy-extracted Δp saturates in about 25 cavity decay times, after $\tau_s = \tau_{sw}$. However, the spectrum at saturation is still rather broad (eleven modes FWHM which corresponds to half the gain bandwidth $N = \epsilon^{-1}$). Continuation of the simulation shows it will eventually settle to a single mode with $p_{inj} \approx 4.2$ after a large number of cavity decay times.

The detuning of the final mode is controlled by the time dependence of the voltage pulse $[p_{inj,0}(\tau_s)]$. As a result of many other simulations we have performed, we conclude that the mode which becomes dominant is the mode for which the rate of change of p_{inj} has become small enough while $p_{inj,n}$ is in the range corresponding to maximum linear growth, $p_{inj,n} \sim 2.606$, to allow for significant growth of the mode. This mode then becomes large enough to suppress its neighbors and remains dominant while $p_{inj,n}$ increases to its final value resulting in high efficiency. If the voltage rise is instantaneous, the mode with maximum linear gain $P_{inj} = 2.606$ dominates. If the rate of approach to the final voltage is too slow, the dominant mode is carried to values of p_{inj} outside (above) the triangle of stable operation. Then a lower frequency satellite of this mode becomes unstable and grows, eventually becoming the dominant mode. The result is that the final state is still a single mode with a value of $p_{inj,n}$ just inside the stability boundary. Fortunately, this state has quite high efficiency; $\Delta p \approx 5.0$ compared with the value realized in the “instant turn on” case $\Delta p = 3.4$.

The time required to reach single-mode equilibrium

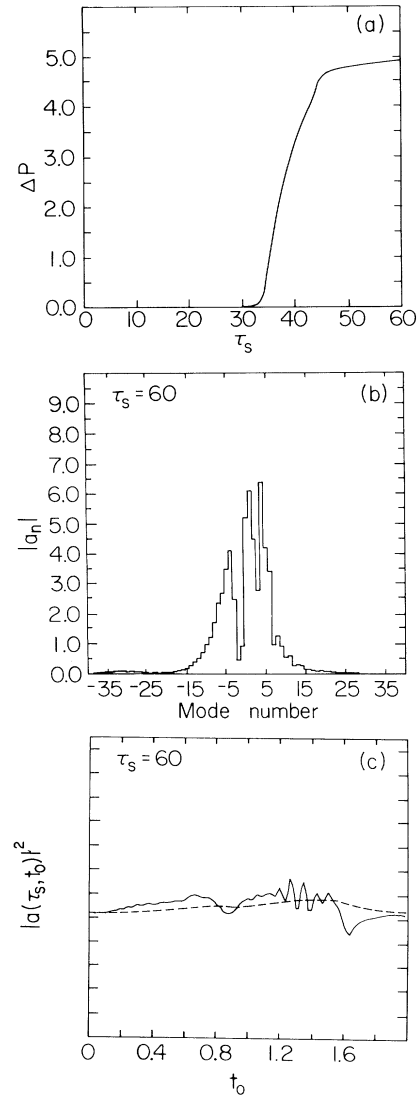


FIG. 2. Sample of a multimode simulation with 81 modes, $\epsilon = 0.05$, $\chi = 3$, and the voltage tapering parameters $p_f = 4.8$, $p_s = 1$, $\tau_{sw} = 20$, and $p_* = 4.5$. (a) The time history of Δp , (b) spectrum at $\tau_s = 60$, and (c) fast time t_0 dependence of $|a(\tau_s, t_0)|^2$ at $\xi = 0$ and $\tau_s = 60$. The dashed line is the same quantity but averaged over time period 0.5.

can be estimated using the same satellite stability calculations of Ref. 7 which produced Fig. 1. There it was shown that the damping rate (in inverse cavity decay times) of the neighboring satellites scales as $(n\epsilon)^2$. Thus, the number M of satellites present after a time τ_s is approximately $M \approx (\epsilon^2 \tau_s)^{-1/2}$. The continuation of our simulation roughly confirms this scaling. Reexpressing this estimate as a real time (t) dependent spectral width gives⁷ $\Delta\omega/\omega \approx 0.5 N_w^{-1} (t_d/t)^{1/2}$, where N_w is the number of wiggles, t_d is the decay time of radiation in the empty cavity, and $t \gg t_d$ and $v_g = c$ are assumed.

The long-lived, weakly damped satellites were shown to correspond to perturbations in the phase and not the magnitude of the radiation field.^{7,11} Thus, the plot of the fast time t_0 dependence of the output power [solid curve in Fig. 2(c)] shows only a small amount of interference in spite of the broad spectrum. The small high-frequency oscillations visible in Fig. 2(c) come from a transient excitation of the side-band instability. These modes are visible on the spectrum plot at $n = -30$ to -35 .

The results of our simulation can be extrapolated in the following way to model the observations of Ref. 12 where the fractional gain bandwidth is 0.3%, the cavity decay time based on 12% per pass power loss is 0.4 μ sec, and single-mode operation was claimed. Our simulation predicts a spectral width in the experiment of $\Delta\omega/\omega \sim 0.15\%$ (half the gain bandwidth). This number is small enough to be masked by the limited resolution of the Fabrey-Perot interferometer and the reported 0.1% shot-to-shot variation in beam energy. The strongest experimental evidence advanced supporting single-mode operation¹² was the relative constancy of a fast diode signal measuring the output power. However, our simulation shows that many modes can be present and still give a constant output signal. This is illustrated in Fig. 2(c) (dashed line) where we have averaged the fast time signal over a time period corresponding to the response time of the fast diode. Thus, we do not believe a single-mode equilibrium was established in the experiment.

In conclusion, we have demonstrated the conditions under which a free-running FEL oscillator will operate in a single mode. In general, the time to reach such a state is extremely long unless some method of external mode control is applied.

This work was supported by the U.S. Department of Energy and the Office of Naval Research. The authors gratefully acknowledge helpful discussions with Dr. V.

Granatstein and Dr. E. Ott.

(a)Also at Departments of Electrical Engineering, and Physics and Astronomy.

¹Ya. L. Bogomolov, V. L. Bratman, N. S. Ginzburg, M. I. Petelin, and A. D. Yanakovsky, *Opt. Commun.* **36** 109 (1981).

²A. Bondeson, B. Levush, W. Manheimer, and E. Ott, *Int. J. Electron.* **53**, 547 (1982).

³In the case of a planar wiggler, ω_s is defined by $\omega_s^2/\omega^2 = 2C(\delta)(qA/mc^2)\kappa(1 + \frac{1}{2}\kappa^2)/\gamma^4\beta_z^2$, where A is the vector potential associated with the radiation field; q , m , γ , and β_z are the charge, mass, relativistic factor, and normalized axial velocity of the electrons, and $\kappa = qB_w/mc^2k_w$ is the wiggler parameter with B_w being the strength of the wiggler field. The coupling coefficient $C(\delta) \approx \frac{1}{2}[J_0(\delta) - J_1(\delta)]$, where J_0 and J_1 are the cylindrical Bessel functions of zero and first order, respectively, and $\delta = \kappa^2/4(1 + \kappa^2/2)$.

⁴The quantity Δp is the difference between the average values of the detuning parameter for electrons as they enter and leave the interaction region, and thus determines the average energy extraction.

⁵T. C. Marshall, *Free Electron Lasers* (MacMillan, New York, 1985), p. 51.

⁶The normalized current is defined by $\hat{I} = (4\pi qj/mc^2\omega k) \times (L\omega/c)^3 4C^2(\delta)\kappa^2(1 + \frac{1}{2}\kappa^2)/(\gamma\beta_z)^5$, where j is the effective current density of the electron beam accounting for appropriate filling factors.

⁷T. M. Antonsen and B. Levush (to be published).

⁸N. M. Kroll, P. L. Morton, and M. N. Rosenbluth, *IEEE J. Quantum Electron.* **17**, 1436 (1981).

⁹W. B. Colson, *J. Soc. Photo-Opt. Instrum. Eng.* **453**, 289 (1983).

¹⁰P. Sprangle, C. M. Tang, and I. Bernstein, *Phys. Rev. Lett.* **50**, 1775 (1983).

¹¹A. P. Chetverikov, *Zh. Tekh. Fiz.* **51**, 2452 (1981) [*Sov. Phys. Tech. Phys.* **26**, 1452 (1981)].

¹²L. R. Elias, G. Ramain, J. Hu, and A. Amir, *Phys. Rev. Lett.* **75**, 424 (1986); L. R. Elias, *IEEE J. Quantum Electron.* **23**, 1470 (1987).